

Photometric Cross-Calibration and Comparison of the SDSS Stripe 82 Standard Stars Catalog with Gaia DR2, Pan-STARRS1, DES and CFIS Catalogs

KARUN THANJAVUR , ¹ ŽELJKO IVEZIĆ , ² SAHAR S. ALLAM , ³ DOUGLAS L. TUCKER , ³ AND J. ALLYN SMITH 

¹Department of Physics & Astronomy, University of Victoria, 3800 Finnerty Road, Victoria, BC V8P 5C2, Canada

²Department of Astronomy and the DiRAC Institute, University of Washington, 3910 15th Avenue NE, Seattle, WA 98195, USA

³Fermi National Accelerator Laboratory, Batavia, IL 60510, USA

⁴Dept. of Physics, Engineering & Astronomy, Austin Peay State University, 601 College St., Clarksville, TN 37044, USA

(Received December 14, 2020; Revised Feb 30, 2022; Accepted Feb 31, 2022)

Submitted to AJ

ABSTRACT

We extend the SDSS Stripe 82 Standard Stars Catalog reported in Ivezić et al. (2007) with post-2007 SDSS imaging data. Our catalog lists averaged SDSS *ugriz* photometry for nearly a million stars brighter than $r \sim 22$ matched with the earlier version of the catalog. However, this new version is based on 2-3 times more measurements per star, resulting in 1.4-1.7 times smaller random errors than in the original catalog, and about three times smaller than those for individual SDSS runs. Random errors in the new catalog are below 0.01 mag for stars brighter than 20.0, 21.0, 21.0, 20.5, and 19.0 in *ugriz*, respectively. We achieve this error threshold by using Gaia DR2 Gmag photometry to derive gray photometric zeropoint corrections, as functions of R.A. and Declination, for the SDSS catalog, and Gaia's BP-RP colors to derive corrections in the *ugiz* bands, relative to the *r* band. We test the quality of recalibrated SDSS photometry by comparing it to Pan-STARRS1, DES and CFIS photometry for the same stars. This multi-survey comparison indicates that the spatial variation of photometric zero points in the updated SDSS catalog is well below 0.01 mag (rms), with typical values of 3-7 millimag in the R.A. direction and 1-2 millimag in the Declination direction, except for the *u* band with a scatter of about 6 millimag. By comparing updated SDSS photometry with synthetic SDSS photometry for three white dwarfs with the HST CalSpec absolute photometry data, we found statistically significant ($> 3\sigma$) AB zeropoint offsets in the *riz* bands, ranging from 0.015 mag to 0.035 mag, while in the *u* and *g* bands we only placed upper limits (at 2σ : 0.038 mag and 0.028 mag, respectively). We also report a few minor photometric problems with all the surveys considered here, including Gaia DR2. Due to its large size and cross-checks with other surveys, this updated SDSS catalog can be used to robustly calibrate or test *ugriz* photometry below 1% level, for example, as needed for the commissioning phase of the Rubin Observatory Legacy Survey of Space and Time.

Keywords: catalogs – instrumentation: photometers – methods: data analysis – standards – surveys – techniques: photometric

1. INTRODUCTION

Modern multi-band photometric sky surveys aim to deliver measurements accurate¹ at the 1% (0.01 mag) level, to enable cosmological and other high-precision measurements (e.g., the Vera Rubin Observatory Legacy Survey of Space and Time, Ivezić et al. 2019). Photometric data are usually calibrated using sets of standard stars whose brightness is known from previous work. One of the largest catalogs with sub-percent measurement precision and optical multi-

Corresponding author: Karun Thanjavur
karun@uvic.ca

¹ Except for zeropoint offsets from the AB magnitude scale, discussed in Section 3.7.

band *ugriz* photometry was constructed by averaging multi-epoch data for about a million stars collected by the Sloan Digital Sky Survey (SDSS, York et al. 2000) in a 300 deg^2 region known as SDSS Stripe 82 (Ivezić et al. 2007, hereafter I007). The SDSS *ugriz* photometric system is now in use at many observatories worldwide and this catalog² (hereafter I007 catalog) has been used both for calibration and testing of other surveys.

After the completion of I007 catalog, SDSS has obtained additional imaging data, about 2-3 times more measurements per star depending on its sky position within Stripe 82. This increased number of data points can result in averaged photometry with 1.4-1.7 times smaller random errors (precision) than in the original catalog (and about three times as small as for individual SDSS runs). In addition, the availability of photometric data from recent wide-field surveys such as the Dark Energy Survey (DES, Dark Energy Survey Collaboration et al. 2016), Pan-STARRS (PS1, Kaiser et al. 2010) and Gaia (Gaia Collaboration et al. 2018), enables a much more detailed and robust cross-calibration, including correcting for residual photometric zeropoint errors in SDSS flat-fielding. For example, Betoule et al. (2013) reported a saw-tooth pattern in photometric residuals between the SDSS and DES catalogs, as a function of Declination (see their Fig. 23). Such a pattern is most likely due to errors in SDSS zeropoint calibration because flat-field correction for Stripe 82 is only a function of Declination (due to drift-scanning in R.A. direction). Given that systematic errors in other catalogs are much smaller (Gaia), or are expected to display different spatial patterns (DES and PS1), it is likely that a cross-comparison of several catalogs can result in significant improvements. These are the main reasons that motivated us to construct an updated version of the SDSS Standard Star Catalog.

We describe datasets used in our analysis in §2, and the construction of the new catalog and its analysis in §3. Our results are summarized and discussed in §4.

2. DATASETS

2.1. SDSS Stripe 82 Imaging Data

In the SDSS survey, Stripe 82 is a contiguous, 300 deg^2 equatorial region, which stretches between $-60^\circ \leq RA \leq 60^\circ$ [20h to 4h], and $-1.266^\circ \leq Dec \leq 1.266^\circ$. Following the initial concerted effort by the SDSS collaboration between 2001 and 2008 to map this region repeatedly to a forecast imaging depth, $r \leq 22$, several other surveys in various wavebands too have targeted this same patch of sky to provide a rich multi-wavelength dataset suitable for a variety of investigations. SDSS observations too have continued in this region (e.g., the SDSS-II search for supernovae, Frieman et al. 2008), resulting in an imaging depth deeper than what was initially planned.

Data from the SDSS imaging camera (Gunn et al. 1998) are collected in drift-scan mode. The images that correspond to the same sky location in each of the five photometric bandpasses (these five images are collected over ~ 5 minutes, with an exposure time of 54 seconds for each band) are grouped together for simultaneous processing as a field. A field is defined as a 36 seconds (1361 pixels) stretch of drift-scanning data from a single column of CCDs (sometimes called a “scan line”; for more details, see I007 and references therein).

2.1.1. The 2007 SDSS Standard Star Catalog

The SDSS standard star catalog published by I007 (version 2.6) was constructed by averaging multiple SDSS photometric observations (at least four per band, with a median of 10) in the *ugriz* system. The catalog includes 1.01 million non-variable unresolved objects. The measurements for individual sources have random photometric errors below 0.01 mag for stars brighter than 19.5, 20.5, 20.5, 20, and 18.5 in *ugriz*, respectively (about twice as good as for individual SDSS runs). Several independent tests of the internal consistency suggested that the spatial variation of photometric zero points is not larger than ~ 0.01 mag (rms).

2.1.2. Post-2007 SDSS data

In this work, we have used the SDSS Data Release 15 (DR15) as available in April 2019 (Blanton et al. 2017). In DR15, the Stripe 82 region is covered by 118 *runs*, which include 32,292 fields, each with observations in the five *ugriz* SDSS filters. Using our programmatic query tool, we obtained the processed data for all these runs from the DR15 public database. In the database, the data are presented as individual FITS tables, named `photoObj_<run>_<camcol>_<field>.fits`. From each fits table, we extracted photometric and astrometric quantities, time of observation, and several ancillary data for all the objects into a formatted, 107-column wide ascii master file for further processing.

² Available from <http://faculty.washington.edu/ivezic/sdss/catalogs/stripe82.html>

The objects in each of these data files were then matched with the standard stars in the I007 catalog using their mean sky positions (R.A. and Declination) and a matching radius of 0.5 arcsec. For matching, only deblended objects ($nchild=0$), lying between rows $64 < objc_rowc < 1424$ in each field, were selected to avoid poor photometry due to blending or lying close to edges of the CCD. From these matched objects, only those with photometric error <0.1 mag were selected to compute photometric zeropoint offsets between the I007 catalog and DR15. These offsets were obtained independently for all runs and fields, and in all five filters, and applied to bring our DR15 based catalog to the same photometric scale as the I007 catalog – in essence, we have re-calibrated photometry for all Stripe 82 runs in DR15 using the I007 catalog. In addition, the MJD and fractional MJD of observation were computed using the median of the TAI values (the GPS based time reported by the SDSS Apache Point Observatory) for these matched objects. In the final step, the photometric, astrometric and other details for each of these matched standard stars were written to independent (one per star) light curve files. Further processing of these light curves is described in Section 3.1.

All these processing steps were completed on a single quad-core desktop needing several days of processing. The final dataset, consisting of all the light curves in the five $ugriz$ filters for the 1,006,849 standard stars in the I007 catalog resulted in ~ 20 GB of tabular data. To make file search and access fast, the data have been chunked into sub-directories, each spanning 1 deg in RA, and 0.1 deg in Dec (a “poor-man’s” two-dimensional tree structure). These light curve data files can be made available as a single tarball by emailing the contact author.

2.2. *Gaia Data Release 2 (DR2) Data*

The second Gaia Data Release, Gaia DR2, includes astrometry, photometry, radial velocities, and information on astrophysical parameters and variability, for approximately 1.7 billion sources (Gaia Collaboration et al. 2018). This dataset is based on the first 22 months of the mission and includes celestial positions and the apparent brightness in the broad-band G (Gmag hereafter) for sources brighter than Gmag ~ 21 . This data release also contains two additional broad-band magnitudes, the BP (330-680 nm) and RP (630-1050 nm).

Gaia DR2 photometry is (**DLT:**) generally superior to ground-based photometry for sources with sufficient signal-to-noise ratio, and we use it to derive zeropoint corrections for SDSS photometry, as described in Section 3.

2.3. *Dark Energy Survey (DES) Data*

The Dark Energy Survey (DES; Dark Energy Survey Collaboration et al. 2016) is an imaging survey of the Southern Galactic Cap in 5 filter passbands ($grizY_{DES}$) that was conducted from 2013 to 2019 with the 570 mega-pixel Dark Energy Camera (DECam; Honscheid & DePoy 2008; Flaugher et al. 2015) on the Victor M. Blanco 4-m telescope at the Cerro Tololo Interamerican Observatory.

For this paper, we made use of the DES Data Release 1 (DES DR1; Abbott et al. 2018) public data set, which is based on the first 3 years of DES observations. The DES DR1 object catalog consists of ~ 400 million objects to a depth of 24.33, 24.08, 23.44, 22.69, 21.44 mag in $ugrizY_{DES}$ ($S/N = 10\sigma$). The DES DR1’s photometric calibration is estimated to be uniform at the sub-percent level (RMS) for each of the five filter passbands over the entirety of the survey footprint. Its astrometric precision is quoted to be 151 milli-arcsec (RMS). We downloaded DES DR1 data via the NOAO Data Lab³ Table Access Protocol (TAP) service, selecting stars in the general area of the SDSS Stripe 82 region of the DES footprint. For the purposes of our analysis, we downloaded the catalog-coadd weighted mean PSF magnitude (WAVG_MAG_PSF) and magnitude error (WAVG_MAGERR_PSF) as well as the number of observations that went into the weighted catalog-coadd weighted mean PSF magnitude (N_EPOCHS) in each filter band for each downloaded DES object. In total, 3 585 229 stars were downloaded in the region ($RA > 270^\circ$ or $< 105^\circ$; $DEC = -3.5^\circ$ to $+3.5^\circ$), of which 619 741 were matched to our SDSS catalog using a match radius of 0.5 arcsec.

2.4. *Pan-STARRS (PS1) Data*

The Panoramic Survey Telescope And Rapid Response System, Telescope 1 (Pan-STARRS-1, or PS1), commissioned in 2010, is the first of planned four 1.8m telescopes designed to map three quarters of the entire sky visible from Hawaii (Kaiser et al. 2010). This panchromatic, synoptic survey, called the 3π Steradian Survey is carried out in five bands, $grizy_{P1}$, with limiting magnitudes of 23.3, 23.2, 23.1, 22.3, and 21.4 mag. Chambers et al. (2016) provide full details about the PS1 observatory, the surveys carried out and the resulting data products, while complete details about the processing and calibrations of the survey are provided in a series of three papers Magnier et al. (2020a,b,c).

³ <http://datalab.noao.edu>

Here we used the 2019 data release PS1-DR2 from *MAST*. The catalog overlapping the Stripe 82 region contains over 7 million point sources taken from the stacked 3π Steradian Survey. From the large set of measured and derived quantities available for these objects, we downloaded $grizy_{P1}$ PSF photometry and various quality flags. For this region, the mean positional uncertainties are 12 and 11 milli-arcsec in the RA and Dec directions. Based on this positional precision and that of our SDSS standard stars catalog, we matched both catalogs using a matching radius of 0.5 arcsec. The resulting matched catalog used in our analysis presented in §3.4 contains 909,000 objects. Taking the r band as being representative, the mean number of visits used to obtain the mean PSF magnitudes for these matched stars is 14.

2.5. Canada-France Imaging Survey (CFIS) Data

The Canada-France Imaging Survey (CFIS) is a large observing program being carried out at the Canada-France-Hawaii Telescope (CFHT) to map the northern sky in the MegaCam u and r bands. With a broad range of science goals, including providing ground-based optical photometry to complement the Euclid space mission, CFIS aims to cover $10,000 \text{ deg}^2$ in the u band to a depth of 24.4 mag. For our analysis, we were provided the u band data which overlaps the Stripe 82 footprint from the CFIS Data Release 2 (DR2, January 2020). In this region, CFIS data are available only for Declination $> +0.45$ degree, thus covering only about a quarter of the Stripe 82 survey footprint.

The available CFIS DR2-Stripe 82 catalog contains close to 965,000 sources, of which $\sim 315,000$ matched within a match radius of 0.5 arcsec with stars in our SDSS standard stars catalog. The astrometry over the complete CFIS survey region has been calibrated against *Gaia* DR1, and has positional uncertainties to $< 0''.034$ arcsec (Ibata et al. 2017). From the matched objects, we select only bright stars, $r \leq 20$ mag, with colors $\leq (u-g)_{SDSS} \leq 2.1$, following Ibata et al. (2017). This color-magnitude cut yields 150,114 stars, which are used in the comparison described in §3.5. We note that that the transmission curve of the MegaCam u band filter used for the CFIS survey differs noticeably from that of the SDSS u band filter (see Figure 2 in Ibata et al. 2017).

2.6. GALEX Data

The Galaxy Evolution Explorer (*GALEX*) all-sky survey catalog in the NUV (1771-2831 Å) and FUV (1344-1786 Å) bands provides a unique photometric dataset to constrain the u -band of a multiband survey such as the SDSS. Processed and calibrated archival data from the eight year, All-sky Imaging (AIS) and Medium depth Imaging (MIS) surveys are available at *MAST*⁴. Due to the failure of the FUV detector midway through the survey, the available imaging depth in this band is shallower by nearly 1 ABmag than the NUV depth of 20.8 ABmag in the AIS. Overall, the source number count in the FUV is, on average, only a tenth of that in the NUV. Given these limitations in the FUV survey, we extracted only sources in the NUV catalog corresponding to the Stripe 82 footprint.

Bianchi et al. (2017) provide full details of the *GALEX* survey, and we summarize only the NUV details, which are pertinent to our analysis here. The survey area had a fairly uniform coverage, leading to total exposure times of ~ 150 s in the AIS, and ~ 1500 s in the MIS. The corresponding NUV survey depths are 20.8 and 22.7 ABmag in the two surveys respectively. Objects in the S82 region were extracted and matched with our SDSS catalog using a matching aperture radius of 3'', which corresponds to the matching radius used internally by *GALEX* to match their NUV and FUV sources. The *GALEX* catalogs do not list the RA, Dec positional errors for their sources, and we found their listed sky positions generally carry a greater uncertainty than the other catalogs used in this work.

Our matched *GALEX* catalog consists of 150945 NUV sources in the S82 footprint for which we obtained NUV aperture magnitudes and uncertainties, as well as various fitted geometric measures for each of them. The astrometry has greater uncertainty than that of SDSS, with mean positional uncertainties of **(DLT:) 1.0'' rms; we also note that there is an overall mean shift in the GALEX astrometry relative to tha of the SDSS by -0.1'' (RA) and +0.3'' (DEC)**. In addition, we find that the available depth in the S82 region is not very deep, with $> 80\%$ of the matched sample brighter than $r=18$ mag.

3. THE CONSTRUCTION AND ANALYSIS OF THE NEW V3.4 CATALOG

We first describe the construction of the new SDSS catalog and derivation of photometric zeropoint corrections using *Gaia* DR2 data, and then compare the resulting photometry to *Gaia* DR2, DES, Pan-STARRS and CFIS catalogs.

⁴ <https://galex.stsci.edu/GR6/>

3.1. The construction of raw SDSS catalog from light curves

Given light curve data files described in Section 2.1.2, we computed the median and mean magnitudes, their formal uncertainties and χ^2 (assuming constant brightness) for all stars, in all five bands. Due to more observational epochs in DR15, the new data are more sensitive to variability; following I007, we applied $\chi^2 > 3$ in the *gri* bands, as well as requirements for at least 4 epochs in the same three bands and the formal uncertainty of the mean *r* band magnitude below 0.05 mag. These selection criteria recovered 98.5% stars from the original catalog, resulting in a new catalog with 991,472 stars.

Figure 1 compares the numbers of epochs for matched stars and their formal uncertainties of the mean *r* band magnitude. The new 2020 catalog has about 2-3 times more measurements per star, depending on its sky position within Stripe 82. Consequently, formal photometric uncertainties (“random errors”) are about 1.4-1.7 times smaller. This raw catalog is labeled version v3.1, and is publicly available from the same website⁵ as the original 2007 catalog.

A star-by-star comparison of the photometry between the old and new catalogs is discussed in Section 3.3.

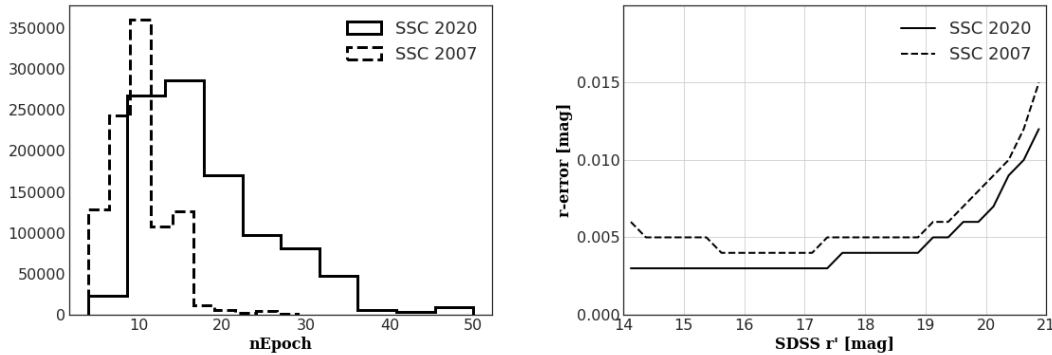


Figure 1. *Left:* A comparison of the number of observational epochs for matched stars in the 2020 versus 2007 Standard Star Catalog (SSC). *Right:* A comparison of the median formal *r* band photometric uncertainties of matched objects in the 2020 versus 2007 SSC, as a function of their mean *r* magnitudes.

3.2. The derivation of photometric zeropoint corrections using Gaia DR2 data

The variation of photometric zeropoints with position on the sky in the I007 catalog (see their eq. 4) was constrained using a combination of stellar colors (the principal axes in color-color diagrams, for details see Ivezić et al. 2004) and a standard star network (Smith et al. 2002; Tucker et al. 2006). It is likely that residual errors in zeropoint calibration (e.g., a saw-tooth pattern, as a function of Declination, was reported by Betoule et al. 2013; see their Fig. 23) can be further minimized using uniformly calibrated space-based photometry from Gaia Data Release 2 (DR2).

3.2.1. Positional matching of the SDSS and Gaia catalogs

Naively, one would positionally match the SDSS and Gaia DR2 catalogs using a matching radius of about 0.3 arcsec because SDSS positions are accurate to better than 0.1 arcsec per coordinate (rms) for sources with $r < 20.5$ mag (Pier et al. 2003). However, observational epochs are sufficiently different that stellar proper motions need to be accounted for; indeed, we find a very strong correlation between the SDSS-Gaia positional differences and proper motions published in the Gaia DR2 catalog (see the left panel in Figure 2). After accounting for proper motions, the positions agree at the level of ~ 28 milliarcsec (robust⁶ rms, per coordinate). The residual differences are dominated by systematic errors in SDSS astrometry because there is no increase of this rms with magnitude (see the right panel in Figure 2), and because the contribution of Gaia’s astrometric measurement uncertainties is negligible. The implied SDSS astrometric accuracy of ~ 28 milliarcsec is substantially better than “ < 0.1 arcsec reported by Pier et al. (2003), but note that here we used positions “averaged” over typically ~ 20 SDSS runs (see the left panel in Figure 1).

⁵ <http://faculty.washington.edu/ivezic/sdss/catalogs/stripe82.html>

⁶ We use robust estimator of standard deviation computed as $\sigma_G = 0.741 * (q_{75} - q_{25})$, where q_{25} and q_{75} are the 25% and 75% quantiles, and the normalization factor 0.741 assures that σ_G is equal to standard deviation for normal (Gaussian) distribution.

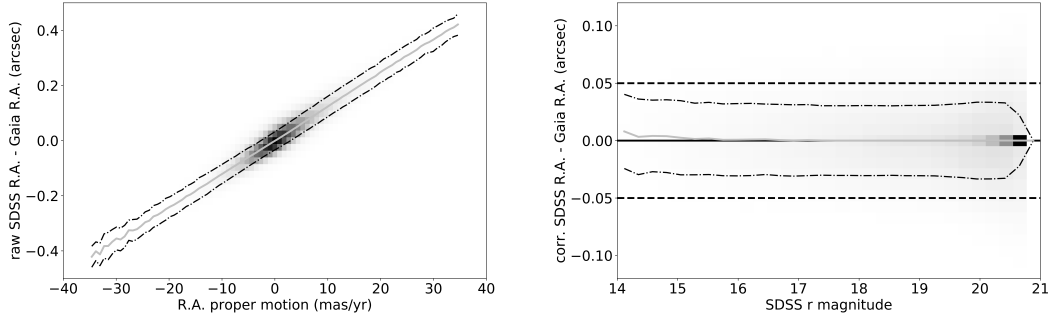


Figure 2. The left panel shows the R.A. difference between SDSS and Gaia vs. R.A. proper motion reported by Gaia DR2. The solid line shows the median difference in bins of proper motion and the dashed lines mark the $\pm\sigma_G$ envelope around the medians, where σ_G is the robust standard deviation. The right panel shows the R.A. difference after correcting using the best-fit R.A. difference vs. proper motion curve, as a function of the SDSS r magnitude. The residual differences are dominated by systematic errors in SDSS astrometry at the level of ~ 28 milliarcsec (note that there is no increase with magnitude). Analogous plots for Declination quantities are similar.

3.2.2. Gaia-based photometric zeropoint corrections

Gaia DR2 reported Gmag magnitudes, which approximately span the SDSS *griz* bandpasses, and BP and RP magnitudes, which approximately correspond to the blue and red halves of the Gmag bandpass. We first used Gmag data to derive “gray” zeropoint corrections (applied to all five SDSS bands), and then use the BP-RP color to derive zeropoint corrections for the *ugiz* bands, relative to the r band.

The basic idea is simple: use Gaia’s Gmag, $\text{Gmag}_{\text{GaiaDR2}}$, and the SDSS *gri* magnitudes to derive synthetic Gmag magnitudes based on SDSS data, $\text{Gmag}_{\text{SDSS}}$; bin the $\Delta\text{Gmag} = (\text{Gmag}_{\text{SDSS}} - \text{Gmag}_{\text{GaiaDR2}})$ residuals by R.A. and Dec, and use the median residuals per bin as the gray correction for SDSS photometry (as functions of R.A. and Dec). Similarly, use Gaia’s BP-RP color to derive synthetic $u-r$, $g-r$, $r-i$ and $r-z$ colors, and used the median residuals per bin as zeropoint corrections for the *ugiz* bands.

Given a large number of matched stars ($\sim 400,000$), and a large number of color combinations, we do not attempt to derive analytic fits for **(DLT:) synthetic** magnitudes and colors but instead use 0.05 mag narrow color bins and linear interpolation between the bins. We have verified that even sixth-order polynomial fits do not provide better results than this simple numerical approach. An example of such a transformation is shown in Figure 3.

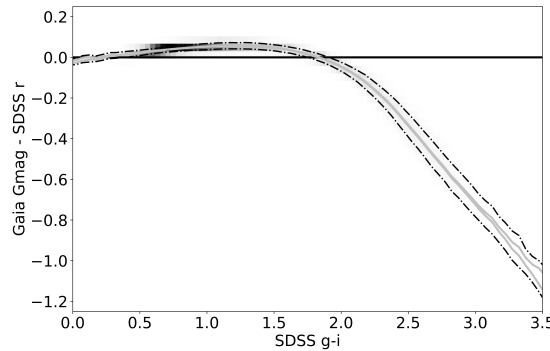


Figure 3. The variation of the difference between Gaia’s Gmag magnitude from Data Release 2 and SDSS r magnitude with the SDSS $g-i$ color. The color map illustrates the distribution of $\sim 393,000$ matched stars with $16 < \text{Gmag} < 19.5$. The two (barely distinguishable) solid lines represent the median values \pm uncertainty of the median for 0.05 mag wide $g-i$ bins. The short-dashed lines show the median values \pm the robust standard deviation for each bin. The horizontal solid line at zero is added to guide the eye. The mean of the two solid lines is used to derive the gray zeropoint correction, as a function of R.A. and Declination.

The variation of Gmag residuals with Gmag (see Figure 4) shows two interesting features. First, there is a sharp “jump” by about 3 millimag at Gmag \sim 16. This jump was a known (and larger problem) in Gaia Data Release 1, but appears not entirely fixed in DR2. The second “feature” is a large ($\sim 0.01 - 0.02$ mag) discrepancy at the faint end: about ~ 10 millimag at Gmag=19.5 and ~ 20 millimag at Gmag=20.5. A comparison of the SDSS catalog with Pan-STARRS and DES catalogs (see Section 3.4 and Figure 15) strongly suggests that the origin of this discrepancy is a bias in Gaia’s Gmag photometry at the faint end, rather than a problem with SDSS catalog (offsets between the SDSS and DES photometry are $< 1 - 2$ millimag at Gmag \sim 20.5).

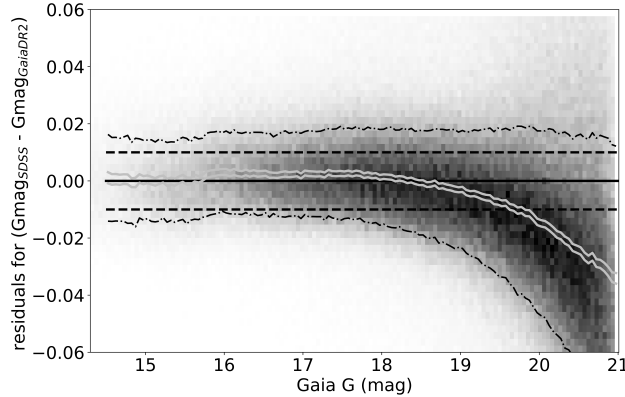


Figure 4. The variation of the residuals between Gaia’s Gmag from Data Release 2 and synthetic Gmag values generated using SDSS *gri* photometry. The two solid lines represent the median values \pm uncertainty of the median for each 0.05 mag wide Gmag bin. The short-dashed lines show the median values \pm the robust standard deviation for each bin. The horizontal solid and long-dashed lines at zero and ± 0.01 mag, respectively, are added to guide the eye. Note the jump by about 3 millimag at Gmag \sim 16 – this jump was a known and larger problem in Gaia Data Release 1, and apparently not entirely fixed in DR2. Note also large ($\sim 0.01 - 0.02$ mag) discrepancy at the faint end – a comparison of the SDSS catalog with Pan-STARRS and DES catalogs (see Figure 15) suggests that its origin is a bias in Gaia’s photometry at the faint end, rather than a problem with SDSS photometry.

Given these two features, we limit the calibration sample to the $16 < \text{Gmag} < 19.5$ magnitude range. We further restrict calibration stars to the $0.4 < g - i < 3.0$ color range (approximately A0 to M5 spectral range), yielding a sample of $\sim 372,000$ stars. The behavior of median Gmag residuals per R.A. and Declination bin is shown in Figures 5 and 6.

Except for a few degrees long region at the edge of Stripe 82 (R.A. $>$ 55 deg), the SDSS photometric zeropoints are remarkably stable with respect to R.A.; the scatter is only 3.5 millimag. On the other hand, there are clear deviations in Declination direction, which clearly map to the 12 scanning strips that fill Stripe 82. We note that discrepancies never exceed 0.01 mag (with a scatter of 6.2 millimag), which was the claimed accuracy of the I007 catalog. Thanks to a large number of stars in the sample, and well calibrated Gaia’s photometric zeropoints across the sky, we can now constrain SDSS zeropoints with a precision of about 1 millimag per 0.01 degree wide Declination bin.

The residuals shown in Figures 5 and 6 are applied as “gray” zeropoint corrections to *ugriz* magnitudes, as functions of R.A. and Declination, to all 991,472 stars in the catalog. This catalog version was labeled v3.1, and it is publicly available⁷.

In the next re-calibration step, we derive synthetic $u - r$, $g - r$, $r - i$ and $r - z$ colors from Gaia’s BP-RP color, using the same binning procedure as we used above for Gmag $-r$ vs. $g - i$ variation (see Figure 3). An example of color residuals is shown in Figure 7. The median residuals per R.A. and Declination bins are then used as zeropoint corrections for the *ugiz* bands. We required that the median offsets for all stars are vanishing and thus photometry in the new catalog is on the same AB scale as the old catalog (for related discussion, see Section 3.7). The robust standard deviation for all zeropoint corrections is listed in Table 1.

⁷ See <http://faculty.washington.edu/ivezic/sdss/catalogs/stripe82.html>

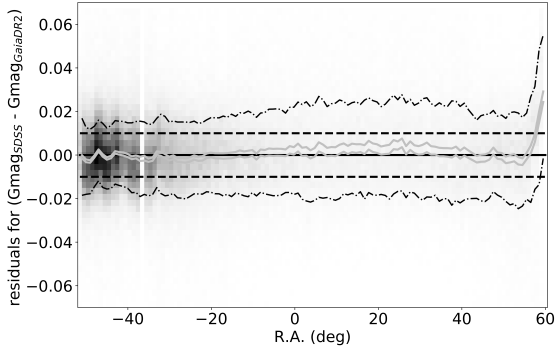


Figure 5. The R.A. variation of the residuals between Gaia’s Gmag from DR2 and synthetic Gmag values generated using SDSS *gri* photometry. The color map illustrates the distribution of $\sim 372,000$ matched stars with $16 < \text{Gmag} < 19.5$ and $0.4 < g - i < 3.0$. The two solid lines represent the median values \pm uncertainty of the median for 1 degree wide R.A. bins. The short-dashed lines show the median values \pm the robust standard deviation for each bin. The horizontal solid and long-dashed lines at zero and ± 0.01 mag, respectively, are added to guide the eye. The mean of the two solid lines is the gray correction, as a function of R.A., applied to the SDSS *ugriz* magnitudes. The standard deviation for the applied correction is 3.5 millimag.

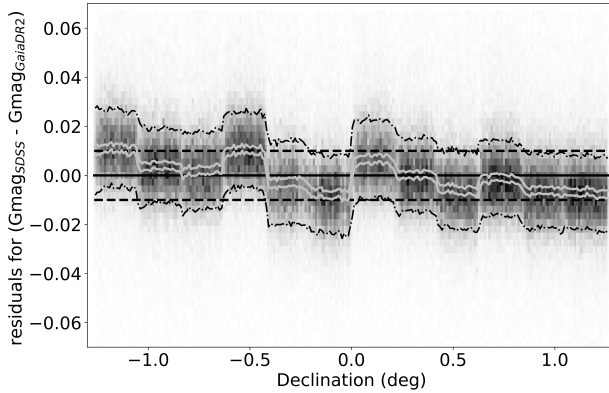


Figure 6. Analogous to Figure 5, except that here results are shown for 0.01 degree wide Declination bins. The 12 clearly visible regions correspond to two SDSS scans (in R.A. direction) and six CCD columns in the SDSS camera. The standard deviation for the applied correction is 6.2 millimag, with a maximum absolute value of ~ 0.01 mag.

The largest corrections were derived for the *u* band. Given that Gaia’s BP-RP color does not strongly constrain the *u* band flux, we used the CFIS catalog (see Section 2.5) as an independent verification test. We verified that zeropoint errors in the SDSS catalog implied by Gaia’s and CFIS data agree at the level a few millimags in Declination direction, but found $\sim 0.01\text{--}0.02$ mag large inconsistencies for R.A. bins. For this reason, we only applied *u* band correction in Declination direction. The plausible *u* band zeropoint errors in the new catalog are further discussed in Section 3.5. This final catalog version was labeled v3.4, and it is also publicly available.

3.2.3. Validation of recalibration

By construction, the new v3.4 catalog should not show appreciable zeropoint residuals when binned by R.A. and Declination. We have verified this expectation for all colors used in recalibration. For illustration, Figure 8 shows such a test for the *g* – *r* color, with binned median scatter of the order 1 millimag.

3.3. Comparison of the SDSS v2.6 and v3.4 catalogs

The v2.6 (“old”) SDSS Standard Star Catalog has been extensively used (e.g., Frieman et al. 2008), and here we briefly analyze differences between the v3.4 (“new”) and v2.6 magnitudes to inform the future users about catalog

Table 1. The robust standard deviation for binned SDSS-based vs. Gaia-based color residuals^a.

Color	rms for R.A.	rms for Dec
gray (Gmag)	3.5	6.2
$u - r$	0.0 ^b	20.4
$g - r$	4.0	4.2
$r - i$	4.1	3.2
$r - z$	7.4	2.9

^aThe standard deviation for applied Gaia-based zeropoint corrections. The robust standard deviation is estimated using interquartile range. The units are millimag.

^bFor the u band, we could not confirm the R.A. behavior of Gaia-based zeropoint correction with the CFIS data and didn't apply it. The large u band correction as a function of Declination was validated with the CFIS data (see Section 3.5).

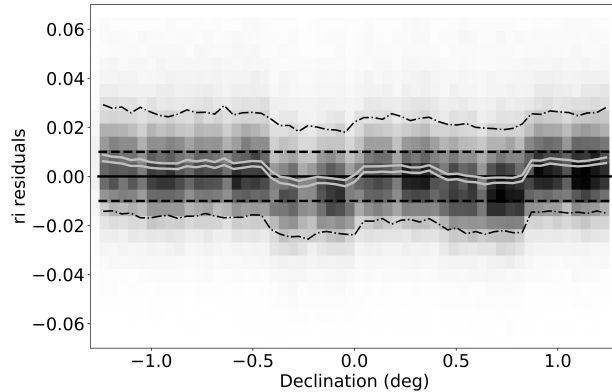


Figure 7. Analogous to Figure 6, except that here residuals correspond to differences between the SDSS $r - i$ color and a synthetic $r - i$ color generated using Gaia's $BP - RP$ color. Note the signature of SDSS camera columns at the level of a few millimags. The standard deviation for the binned medians is 3.2 millimag (for other bands, please see Table 1).

consistency. In our analysis, we first compare v2.6 and v3.4 magnitudes of individual stars and bin the differences by R.A., Declination and magnitude.

On average, both catalog versions are on the same magnitude scale (the median $ugriz$ magnitude differences for all stars are zero by construction). There are no systematic offsets when binned by magnitude, as illustrated in Figure 9. The most obvious differences appear when magnitude differences are binned by Declination. An example is shown in Figure 10, where the periodicity of residuals corresponds to the field-of-view size for the SDSS Photometric Telescope (Tucker et al. 2006). The standard deviation for median values per bin is 6.8 millimag, with extreme values about 0.01 mag. It is likely that systematic errors in the calibration star network photometry were propagated through “flat-field corrections” discussed by I007 to the v2.6 catalog. We note that these errors, now found thanks to Gaia catalogs, are well within the claimed photometric accuracy by both I007 and Smith et al. (2002). The standard deviation for median values per bin for all bands and both coordinates is listed in Table 2.

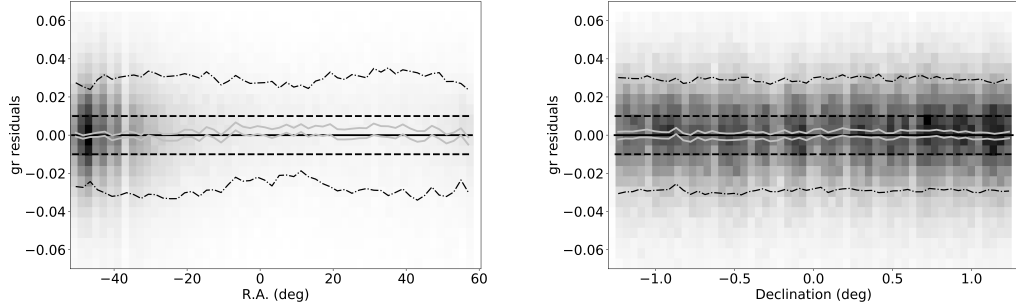


Figure 8. Left: analogous to Figure 5, except that here residuals between the SDSS $g - r$ color from the v3.4 catalog and a synthetic $g - r$ color generated using Gaia’s $BP - RP$ color are shown. The binned median scatter is 1.6 millimag. Right: the $g - r$ residuals are shown as a function of Declination. The binned median scatter is 0.8 millimag.

Table 2. The robust standard deviation for magnitude differences between the v2.6 (old) and v3.4 (new) catalogs.

Band	rms for R.A.	rms for Dec
u	2.3 ^a	25.5
g	4.5	9.4
r	2.0	7.0
i	5.3	6.5
z	8.9	8.4

^aFor the u band, the scatter in R.A. direction is due to more observations in v3.4 than in v2.6, rather than zero-point correction.

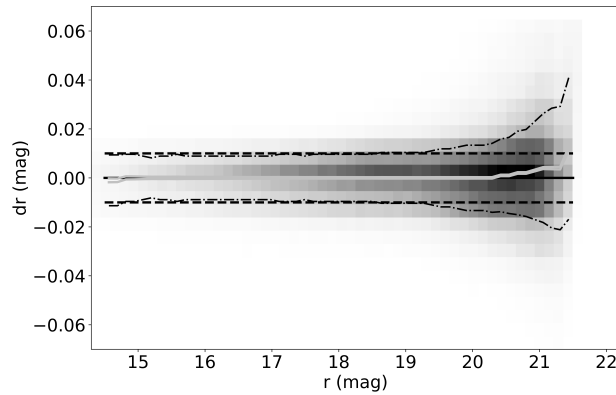


Figure 9. Analogous to Figure 10, except that here the r band differences are shown as a function of the r band magnitude. The scattered of median values per bin is 1.9 millimag. The scatter of individual values is ~ 0.01 mag for $r < 20$, and it is due to more data in the new catalog.

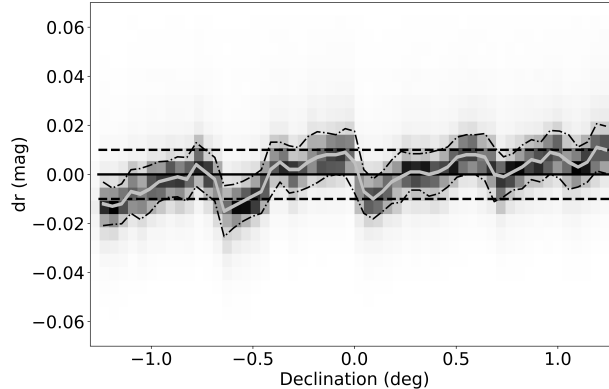


Figure 10. The differences between r band magnitudes listed in the v2.6 and v3.4 SDSS Standard Star catalogs. The size of the four regions corresponds to the field-of-view size of the SDSS Photometric Telescope. The standard deviation for median values per bin is 6.8 millimag, with extreme values about 0.01 mag. The scatter of binned medians in R.A. direction is much smaller – 2.0 millimag. For statistics in other bands, please see Table 2.

Given the quality of Gaia photometry, there should be no doubt that SDSS *ugriz* photometry reported in the new v.3.4 catalog is superior to the old v2.6 catalog. Nevertheless, we perform additional tests, based on the position of the stellar locus in the $g - r$ vs. $u - g$, $r - i$ vs. $g - r$ and $i - z$ vs. $r - i$ color-color diagrams (Ivezić et al. 2004). The tests are based on the second principal color for the blue part of the stellar locus, whose median should not deviate from zero by construction. Figure 11 compares the behavior of the w color for the old v2.6 and new v3.4 catalog and demonstrates that the *gri* photometry is better calibrated in the latter. The behavior of the s and y colors for the new catalog is shown in Figure 12. *Based on these tests, we find that the contribution of the zeropoint errors is < 5 millimag to gri photometry, and < 10 millimag for the u and z bands.*

3.4. Comparison of the new v3.4 SDSS catalog with DES and Pan-STARRS catalogs

The quality of photometric zeropoint calibration for the new SDSS catalog can be conveniently tested with the DES (see Section 2.3) and Pan-STARRS (see Section 2.4) catalogs. Both catalogs list *griz* photometry of sufficient precision for essentially all stars from Stripe 82. Their photometric calibration procedures are expected to result in different spatial patterns and thus a cross-comparison with the v3.4 catalog can reveal residual problems with zeropoint calibration. They are also deeper than Gaia DR2 catalog and thus can provide further clues about the Gmag discrepancy at Gaia’s faint end illustrated in Figure 4.

Our comparison of the magnitude differences is illustrated in Figures 13 and 14, and the robust standard deviation for binned median magnitude differences is listed in Table 3. This multi-survey comparison indicates that the spatial variation of photometric zero points in the updated SDSS catalog is well below 0.01 mag (rms), with typical values of 3-7 millimag in the R.A. direction and 1-2 millimag in the Declination direction. As discernible in the two bottom panels in Figure 13, there are systematic residual errors in the z band zeropoint as a function of Declination at the level of a few millimag. Note also implied DES z band zeropoint errors of up to 0.01-0.02 mag, as a function of R.A. (see the bottom left panel in Figure 13) (**DLT:**), although a similar trend in the equivalent Pan-STARRS plot (bottom right panel in Figure 13) may indicate some of the issue may also reside with the Gaia DR2 calibrations upon which the SDSS Stripee82 calibrations are based.⁸

The variation of the magnitude differences with magnitude (see Figure 15) shows good agreement (to within \sim 5 millimag) even at the faint end ($20 < r < 21$), where Gaia Gmag magnitudes appear too faint by about 0.02 mag, and thus demonstrates a likely problem with Gaia DR2 photometry.

3.5. Comparison of the new v3.4 SDSS catalog and u band data from the CFIS catalog

⁸ For a comparison of DES DR1 and Gaia DR2 calibrations, see, e.g., Fig. 9 of Abbott et al. (2018).

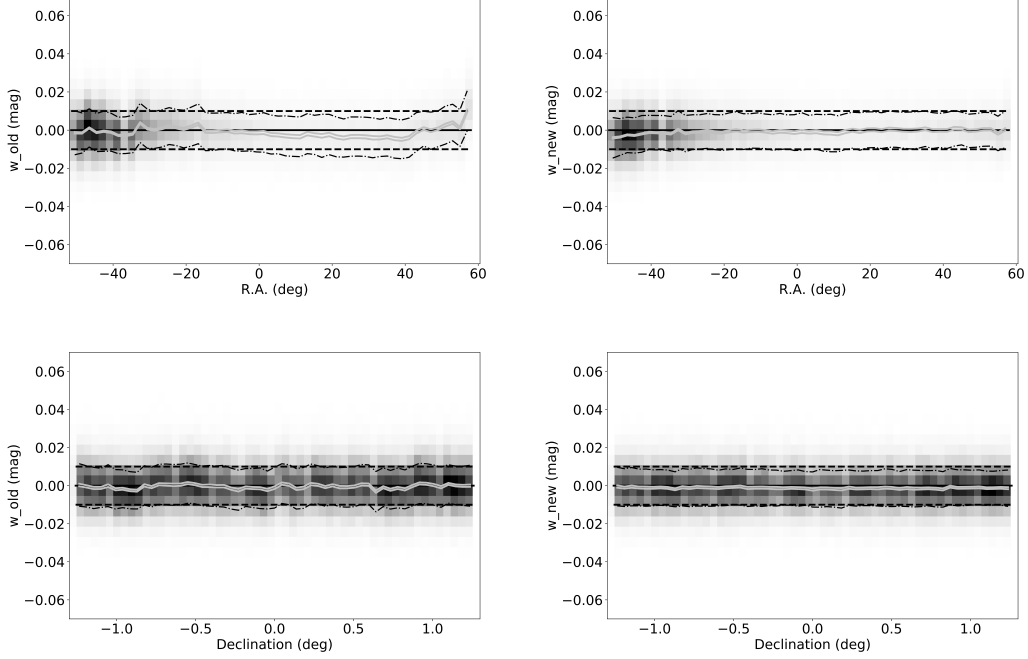


Figure 11. A comparison of the w color, the second principal color in the SDSS $r - i$ vs. $g - r$ color-color diagram, behavior for the v2.6 (left) and v3.4 (right) catalogs. The standard deviation of the median w values binned by R.A. and Dec is 2.6 millimag and 1.1 millimag for v2.6 and 1.0 millimag and 0.3 millimag for v3.4, respectively.

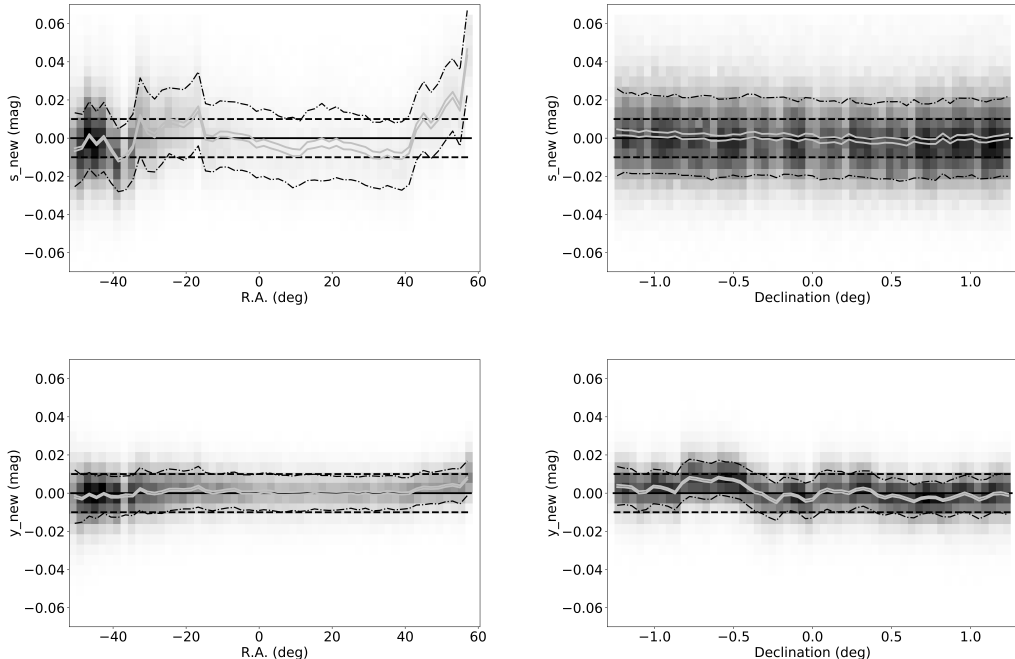


Figure 12. The behavior of the s color (top two panels), the second principal color in the SDSS $g - r$ vs. $u - g$ color-color diagram, and the y color (bottom two panels), the second principal color in the SDSS $i - z$ vs. $r - i$ color-color diagram, for the new v3.4 catalog. The standard deviation of the median s values binned by R.A. and Declination is 9.8 millimag and 1.3 millimag, respectively, and 1.8 millimag and 3.4 millimag for the y color.

Table 3. The robust standard deviation for binned median magnitude differences between the new v3.4 SDSS catalog, and DES and Pan-STARRS1 (PS1) catalogs (millimag).

Band	DES R.A.	DES Dec	PS1 R.A.	PS1 Dec
<i>g</i>	5.1	1.8	3.4	1.4
<i>r</i>	4.1	0.8	2.6	0.7
<i>i</i>	7.3	1.6	3.2	1.0
<i>z</i>	13.6	3.6	6.8	2.3

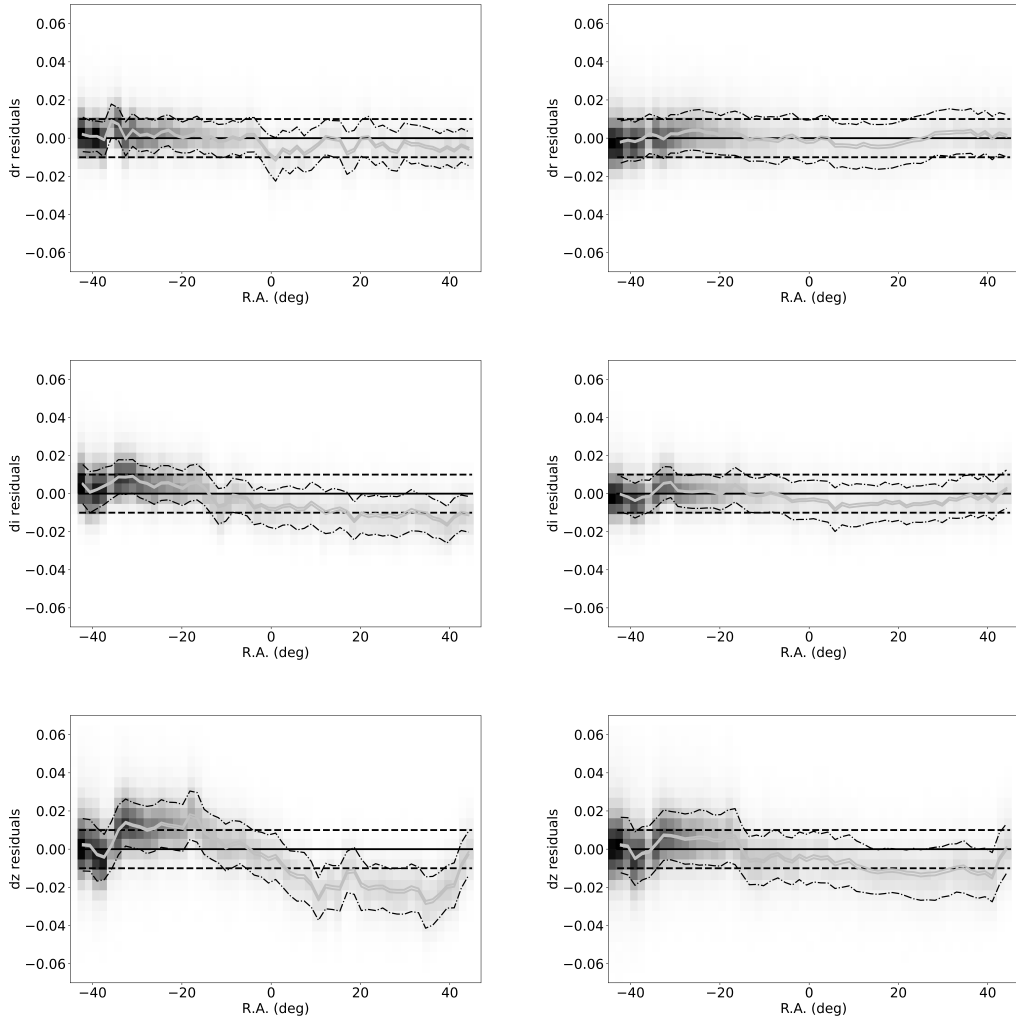


Figure 13. A comparison of the magnitude differences between the SDSS v3.4 catalog and DES (left) and Pan-STARRS (right) catalogs, for the *riz* bands.

The comparison of the new SDSS catalog with the DES and Pan-STARRS catalogs in the previous section did not include the *u* band. To assess the quality of *u* band zeropoint calibration, we use the CFIS catalog (see Section 2.5). The CFIS *u* band photometry was calibrated using a combination of the SDSS, Pan-STARRS and GALEX UV data.

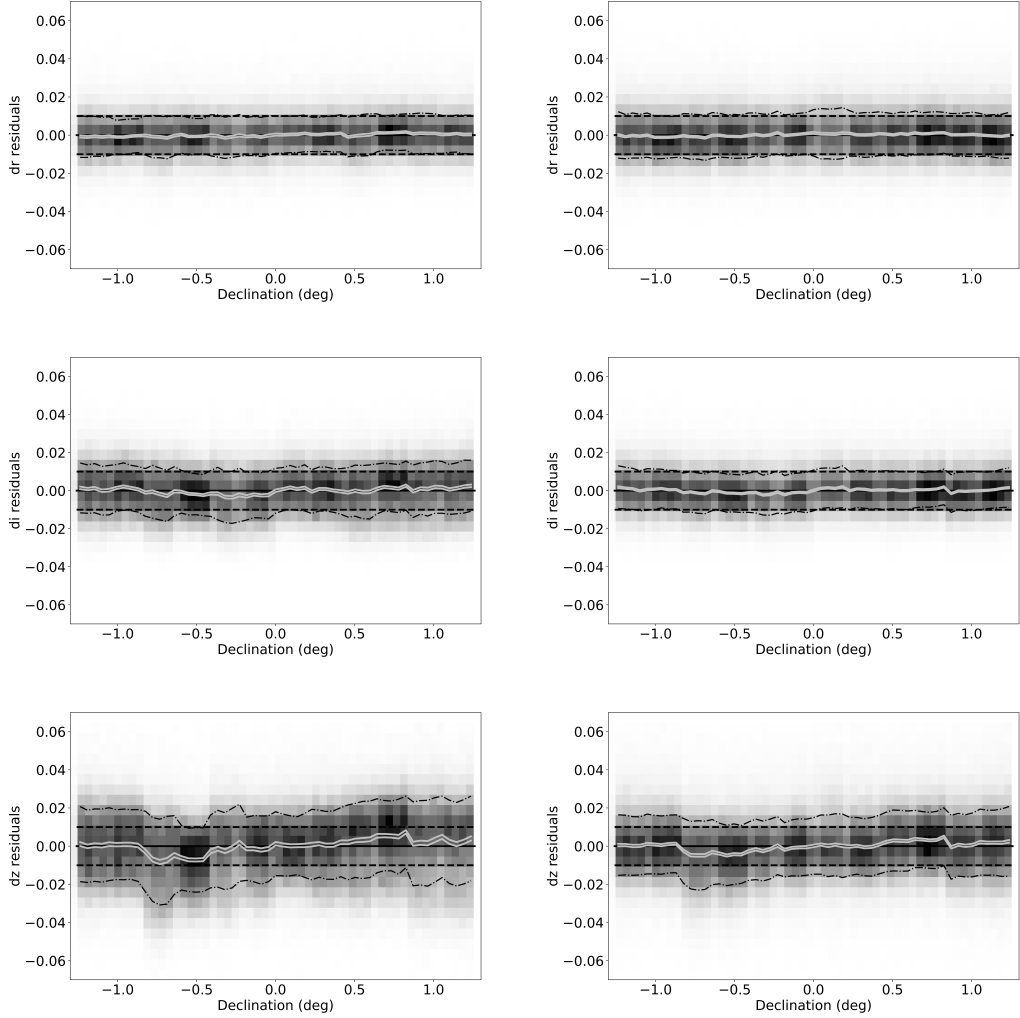


Figure 14. Analogous to Figure 13, except that magnitude differences are binned by Declination.

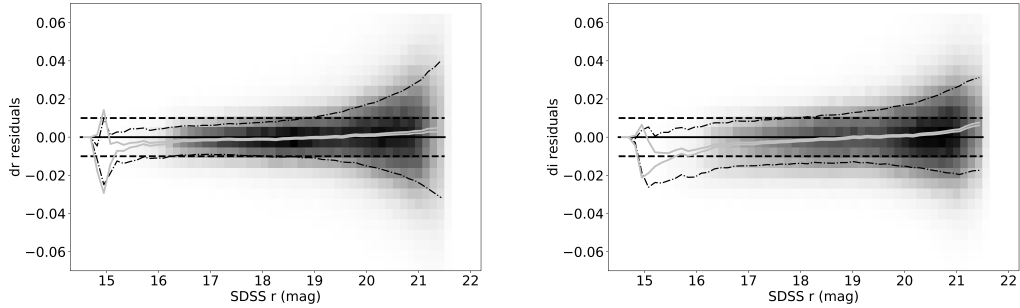


Figure 15. A comparison of the magnitude differences between the SDSS v3.4 catalog and DES catalog, for the r and i bands. Note the good agreement even at the faint end ($20 < r < 21$), where Gaia Gmag magnitudes appear too faint by about 0.02 mag (see Figure 4).

Given that we recalibrated the new SDSS catalog using Gaia data, for this comparison it shouldn't matter that SDSS

data were used in calibration of the CFIS catalog. Nevertheless, the results of this section should be treated with caution.

A star-by-star comparison for about 150,000 sufficiently bright stars ($r < 20$), with colors matching the main sequence ($1.0 < u - g < 2.1$) is illustrated in Figure 16. The binned median scatter for Declination direction is 5.7 millimag with systematic differences of up to about 0.01 mag. The constraints in R.A. direction are more noisy, with residuals appearing about twice as large as in Declination direction. These residuals compare favorably to the results of analysis by Ibata et al. (2017), who showed that some SDSS runs in Data Release 13 have u -band zeropoint errors as large as 0.05 mag.

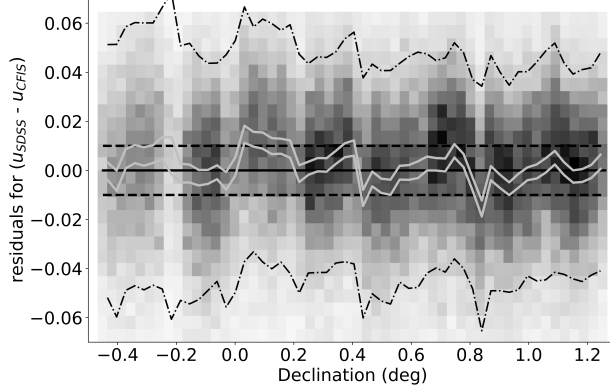


Figure 16. Analogous to Figure 6, except that here residuals between the SDSS u band magnitudes and u band magnitudes from the CFIS catalog (corrected for small color terms, ~ 0.05 mag, as a function of the $u - g$ color), for $\sim 150,000$ matched stars with $1.0 < u - g < 2.1$ and $r < 20$ are shown. The binned median scatter is 5.7 millimag. Note that the CFIS data are available only for Declination > -0.45 degree.

3.6. Comparison of the new v3.4 SDSS catalog and transformed nUV data from the GALEX catalog

We also use the NUV magnitudes from GALEX (see Section 2.6) to provide an independent check on the SDSS u -band magnitudes, following the zeropoint corrections with Gaia photometry described in §3.2. For this we derive the following GALEX to SDSS u transformation equation:

$$\begin{aligned} u_{est} = & NUV_{galex} - 0.999 \times (NUV_{galex} - g_{sdss}) + 0.015 \times (NUV_{galex} - g_{sdss})^2 \\ & - 0.426 \times (g_{sdss} - i_{sdss}) + 0.821 * (g_{sdss} - i_{sdss})^2 + 0.939 \\ & + T \times [-1.233 \times (E(B - V) - 0.15) + 3.430 \times (E(B - V) - 0.15)^2] \end{aligned} \quad (1)$$

where T is a step function in the value of the interstellar reddening, $E(B - V)$, from the Schlegel et al. (1998) reddening map:

$$T(E(B - V)) = \begin{cases} 0 & E(B - V) \leq 0.15 \\ 1 & 0.15 < E(B - V) < 0.3 \end{cases} \quad (2)$$

This transformation relation, which is suitable for stars with $0.5 < (u - g)_{sdss} < 2.0$, $0.2 < (g - r)_{sdss} < 0.8$, $0.3 < (g - i)_{sdss} < 1.0$, and $E(B - V) < 0.3$, has a per star RMS of $\sigma = 0.060$ mag (the relatively high RMS is due in part to the relatively high RMS in the GALEX NUV magnitudes). This relation converts the GALEX NUV magnitudes in to very reasonable approximations of the SDSS u -band. To refine these approximations, we then applied the same sort of numerical transformation that was used for the SDSS/Gaia transformation in Figure 3; this improved the overall per star RMS to $\sigma = 0.050$, with most of the improvement occurring for the bluest ($(u - g)_{sdss} \lesssim 1.0$) and the reddest ($(u - g)_{sdss} \gtrsim 1.0$) stars in our sample.

Despite the relatively noisy results, we can make several conclusions based upon the binned data consisting of 54,660 matches between the v3.4 SDSS catalog and the GALEX catalog. First, in Figure 17, we show the difference between

the SDSS-measured and GALEX-predicted u_{sdss} vs. SDSS u_{sdss} . Although the relation, even when binned like here, is noisy, no obvious strong trends are seen in this plot. Second, in Figure 18, we plot this magnitude difference vs. RA along SDSS Stripe 82. Here, a noticeable large-scale trend can indeed be seen at the ~ 0.01 - 0.02 mag level. It is interesting that these trends in u are qualitatively similar – but opposite in sign – to some of the trends seen in the comparison plots with DES and Pan-STARRS1 in Section 3.4 (see, e.g., Fig. 13). (**DLT: Check this!**). Finally, in Figure 19, we plot this magnitude difference vs. DEC across SDSS Stripe82. Unlike for the CFIS comparison in the previous section (see, e.g., Fig. 16), the GALEX comparison covers the full DEC range of Stripe 82. Overall, there appear to be no obvious large-scale trends. The hints of smaller scale ($\sim 0.4^\circ$) variations – roughly on the scale of an SDSS camera column – seen in the CFIS comparison (Fig. 16), however, are not seen here, likely due to the relative “noisiness” of the GALEX comparison.

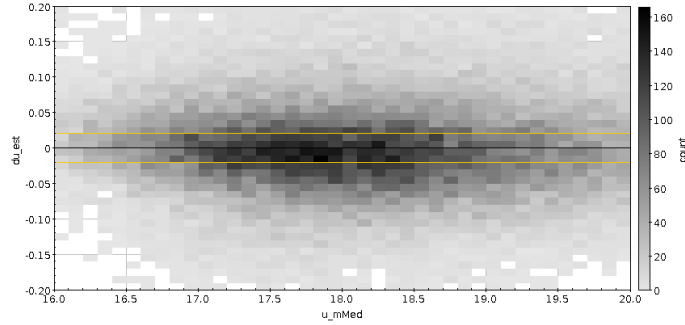


Figure 17. Analogous to Figure 4, except that here residuals between the SDSS u band magnitudes and predicted u band magnitudes transformed from the GALEX catalog are shown. The binned median scatter is Z.Z millimag. (**DLT: replace with jupyternotebook-generate figure when available.**)

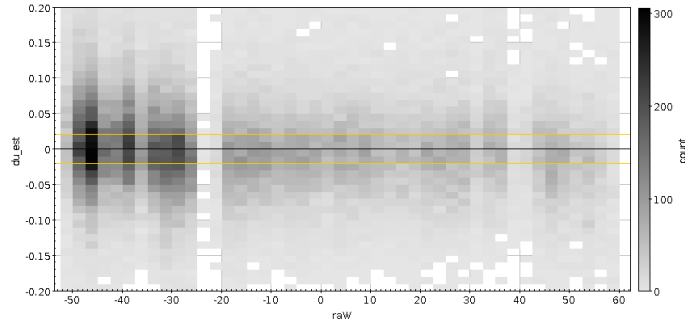


Figure 18. Analogous to Figure 5, except that here residuals between the SDSS u band magnitudes and predicted u band magnitudes transformed from the GALEX catalog are shown. The binned median scatter is Z.Z millimag. (**DLT: replace with jupyternotebook-generate figure when available.**)

3.7. Offsets from AB magnitude scale

We estimate offsets from AB magnitude scale using photometry from three DA white dwarfs observed by HST (see Table 4): GD50 (specifically, the calibrated spectrum file `gd50_004.fits`) from the HST CalSpec database of spectrophotometric standard stars (?)⁹, and SDSSJ 232941.32+001107.8 and SDSSJ 010322.19-002047.7 from ? (the flux-calibrated modeled spectrum files provided by G. Narayan, private communication). These three spectrophotometric calibrators are particularly useful for our purposes since they are faint enough not to be saturated in the SDSS photometry ($r > 14$) and they lie within the SDSS Stripe 82 footprint, making direct comparison to the SDSS measurements relatively simple. Synthetic AB magnitudes for these three DA white dwarfs was accomplished via numerical integration of Equation 8 of ?, which serves to define broad-band AB magnitudes. This equation requires

⁹ <https://www.stsci.edu/hst/instrumentation/reference-data-for-calibration-and-tools/astronomical-catalogs/calspec>

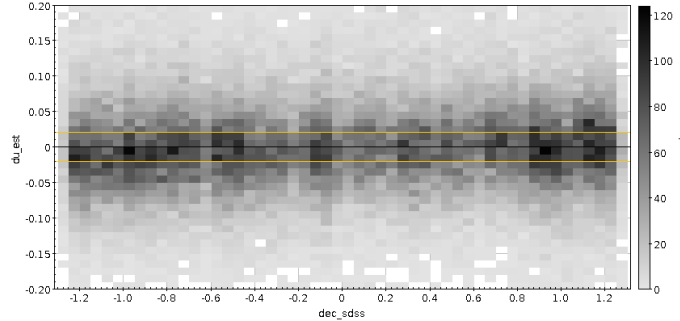


Figure 19. Analogous to Figure 6, except that here residuals between the SDSS u band magnitudes and predicted u band magnitudes transformed from the GALEX catalog are shown. The binned median scatter is Z.Z millimag. (DLT: replace with jupyter notebook-generate figure when available.)

not only a well-calibrated spectrum, but also the well-calibrated bandpass response curves for the photometric system in question. Here, we make use of the SDSS bandpass response curves from Table 4 of ?. Our results for the synthetic SDSS AB magnitudes for these three stars can be found in Table 4. The errors on these synthetic AB magnitudes are expected to be $\sim 0.5 - 1.0$ mag (statistical) and ~ 0.01 mag (systematic). (DLT: Reference???)

Table 5 presents numerical summary of the comparison between SDSS magnitudes and HST-based synthetic magnitudes for three white dwarfs. We used unweighted mean because formal uncertainties for SDSS photometry are subdominant to systematic errors in HST-based synthetic magnitudes, estimated at about 0.01 mag. Uncertainty of the mean offsets was computed from the observed scatter of three values. In the riz bands we detect significant ($> 3\sigma$) deviations, ranging from 0.015 mag to 0.035 mag, while in the u and g bands we can only place upper limits (at 2σ : 0.038 mag and 0.028 mag, respectively).

Table 4. Synthetic SDSS magnitudes for three WD dwarfs with HST photometry^a.

Name	R.A.	Dec.	u	g	r	i	z
GD50	57.2091083	-0.975636	13.409	13.784	14.295	14.655	...
SDSSJ 232941.32+001107.8	352.4221875	0.185500	18.154	18.145	18.466	18.754	19.042
SDSSJ 010322.19-002047.7	15.8424625	-0.346592	18.627	19.057	19.558	19.923	20.258

^aGive here reference to HST data, or some other comment?

^bThe CalSpec spectrum stopped at about 9000 Å and thus did not cover all of SDSS z band.

Table 5. AB offsets implied by three WD dwarfs with HST photometry^a.

	Δu	Δg	Δr	Δi	Δz
mean	-0.009	0.000	0.015	0.016	0.035
σ_{mean}	0.019	0.014	0.004	0.004	0.011

^aOffsets are defined as additive corrections to SDSS photometry to place it on AB scale (in mag). Listed values are unweighted mean and its uncertainty.

4. DISCUSSION AND CONCLUSIONS

To enable further progress in cosmological and other high-precision photometric measurements, modern multi-band photometric sky surveys aim to deliver measurements accurate at the 1% (0.01 mag) level. Over the last decade a number of such large-scale surveys approached, and often exceeded this photometric accuracy threshold. For ground-based surveys, that are affected by variable atmospheric effects and hardware responses to changes in local environment (e.g. temperature), significant improvements can be achieved by averaging multiple observations.

In this paper, we have described the construction and tests of an updated version of the so-called SDSS Stripe 82 Standard Star catalog (Ivezić et al. 2007) that lists averaged SDSS photometry for about a million non-variable stars. Additional post-2007 SDSS data include about 2-3 times more measurements per star than in the original catalog, resulting in 1.4-1.7 times smaller random photometric errors (precision) than in the original catalog, and about three times as small as for individual SDSS runs.

Thanks to the availability of photometric data from recent wide-field surveys (Gaia, DES, Pan-STARRS and CFIS), we were able to derive robust zeropoint corrections and establish that this new catalog is superior to the original catalog. Using a combination of comparison to other catalogs and astrophysical constraints, we find that the contribution of the zeropoint errors to photometric uncertainties is < 5 millimag for the *gri* bands, and < 10 millimag for the *u* and *z* bands.

Various catalog cross-comparisons have revealed minor problems with all the analyzed catalogs. For example, we detected DES *z* band zeropoint errors of up to 0.01-0.02 mag, as a function of R.A., and demonstrated that Gaia Gmag magnitudes appear too faint by about 0.02 mag at Gmag ~ 20 .

We constrained offsets from the absolute AB magnitude scale using three white dwarfs with the HST CalSpec absolute photometry data. In the *riz* bands we measured significant ($> 3\sigma$) deviations, ranging from 0.015 mag to 0.035 mag (see Table 5), while in the *u* and *g* bands we only placed upper limits (at 2σ : 0.038 mag and 0.028 mag, respectively). These constraints on absolute AB magnitude scale could be improved by extend the number of such calibrators.

Thanks to its high stellar density, about 1 star per square arcmin, and demonstrated sub-percent internal photometric precision, this catalog is a good resource for both calibrating and testing other surveys. In particular, it will enable high-precision photometric testing of data collected during the commissioning phase of the Rubin Observatory Legacy Survey of Space and Time.

ACKNOWLEDGMENTS

We thank Stephen Gwyn for providing the CFIS catalog to us, and for discussions of the *u* band photometry.

Funding for the SDSS and SDSS-II has been provided by the Alfred P. Sloan Foundation, the Participating Institutions, the National Science Foundation, the US Department of Energy, the National Aeronautics and Space Administration, the Japanese Monbukagakusho, the Max Planck Society, and the Higher Education Funding Council for England. The SDSS Web site is <http://www.sdss.org>.

Facilities: SDSS, Pan-STARRS, DECam, CFHT

Software: numpy (Oliphant 2006), matplotlib (Hunter 2007), scipy (Jones et al. 2001–), astropy (Astropy Collaboration et al. 2013, 2018), astroML (VanderPlas et al. 2012).

REFERENCES

- Abbott, T. M. C., Abdalla, F. B., Allam, S., et al. 2018, ApJS, 239, 18, doi: [10.3847/1538-4365/aae9f0](https://doi.org/10.3847/1538-4365/aae9f0)
- Astropy Collaboration, Robitaille, T. P., Tollerud, E. J., et al. 2013, A&A, 558, A33, doi: [10.1051/0004-6361/201322068](https://doi.org/10.1051/0004-6361/201322068)
- Astropy Collaboration, Price-Whelan, A. M., Sipőcz, B. M., et al. 2018, AJ, 156, 123, doi: [10.3847/1538-3881/aabc4f](https://doi.org/10.3847/1538-3881/aabc4f)
- Betoule, M., Marriner, J., Regnault, N., et al. 2013, A&A, 552, A124, doi: [10.1051/0004-6361/201220610](https://doi.org/10.1051/0004-6361/201220610)
- Bianchi, L., Shiao, B., & Thilker, D. 2017, ApJS, 230, 24, doi: [10.3847/1538-4365/aa7053](https://doi.org/10.3847/1538-4365/aa7053)
- Blanton, M. R., Bershadsky, M. A., Abolfathi, B., et al. 2017, AJ, 154, 28, doi: [10.3847/1538-3881/aa7567](https://doi.org/10.3847/1538-3881/aa7567)

- Chambers, K. C., Magnier, E. A., Metcalfe, N., et al. 2016, arXiv e-prints, arXiv:1612.05560.
<https://arxiv.org/abs/1612.05560>
- Dark Energy Survey Collaboration, Abbott, T., Abdalla, F. B., et al. 2016, MNRAS, 460, 1270, doi: [10.1093/mnras/stw641](https://doi.org/10.1093/mnras/stw641)
- Flaugher, B., Diehl, H. T., Honscheid, K., et al. 2015, AJ, 150, 150, doi: [10.1088/0004-6256/150/5/150](https://doi.org/10.1088/0004-6256/150/5/150)
- Frieman, J. A., Bassett, B., Becker, A., et al. 2008, AJ, 135, 338, doi: [10.1088/0004-6256/135/1/338](https://doi.org/10.1088/0004-6256/135/1/338)
- Gaia Collaboration, Brown, A. G. A., Vallenari, A., et al. 2018, A&A, 616, A1, doi: [10.1051/0004-6361/201833051](https://doi.org/10.1051/0004-6361/201833051)
- Gunn, J. E., Carr, M., Rockosi, C., et al. 1998, AJ, 116, 3040, doi: [10.1086/300645](https://doi.org/10.1086/300645)
- Honscheid, K., & DePoy, D. L. 2008, arXiv e-prints, arXiv:0810.3600. <https://arxiv.org/abs/0810.3600>
- Hunter, J. D. 2007, Computing in Science & Engineering, 9, 90, doi: [10.1109/MCSE.2007.55](https://doi.org/10.1109/MCSE.2007.55)
- Ibata, R. A., McConnachie, A., Cuillandre, J.-C., et al. 2017, ApJ, 848, 128, doi: [10.3847/1538-4357/aa855c](https://doi.org/10.3847/1538-4357/aa855c)
- Ivezic, Ž., Lupton, R. H., Schlegel, D., et al. 2004, Astronomische Nachrichten, 325, 583, doi: [10.1002/asna.200410285](https://doi.org/10.1002/asna.200410285)
- Ivezic, Ž., Smith, J. A., Miknaitis, G., et al. 2007, AJ, 134, 973
- Ivezic, Ž., Kahn, S. M., Tyson, J. A., et al. 2019, ApJ, 873, 111, doi: [10.3847/1538-4357/ab042c](https://doi.org/10.3847/1538-4357/ab042c)
- Jones, E., Oliphant, T., Peterson, P., et al. 2001–, SciPy: Open source scientific tools for Python.
<http://www.scipy.org/>
- Kaiser, N., Burgett, W., Chambers, K., et al. 2010, in Society of Photo-Optical Instrumentation Engineers (SPIE) Conference Series, Vol. 7733, Ground-based and Airborne Telescopes III, 77330E, doi: [10.1117/12.859188](https://doi.org/10.1117/12.859188)
- Magnier, E. A., Chambers, K. C., Flewelling, H. A., et al. 2020a, ApJS, 251, 3, doi: [10.3847/1538-4365/abb829](https://doi.org/10.3847/1538-4365/abb829)
- Magnier, E. A., Sweeney, W. E., Chambers, K. C., et al. 2020b, ApJS, 251, 5, doi: [10.3847/1538-4365/abb82c](https://doi.org/10.3847/1538-4365/abb82c)
- Magnier, E. A., Schlafly, E. F., Finkbeiner, D. P., et al. 2020c, ApJS, 251, 6, doi: [10.3847/1538-4365/abb82a](https://doi.org/10.3847/1538-4365/abb82a)
- Oliphant, T. E. 2006, A guide to NumPy, Vol. 1 (Trelgol Publishing USA)
- Pier, J. R., Munn, J. A., Hindsley, R. B., et al. 2003, AJ, 125, 1559, doi: [10.1086/346138](https://doi.org/10.1086/346138)
- Schlegel, D. J., Finkbeiner, D. P., & Davis, M. 1998, ApJ, 500, 525, doi: [10.1086/305772](https://doi.org/10.1086/305772)
- Smith, J. A., Tucker, D. L., Kent, S., et al. 2002, AJ, 123, 2121, doi: [10.1086/339311](https://doi.org/10.1086/339311)
- Tucker, D. L., Kent, S., Richmond, M. W., et al. 2006, Astronomische Nachrichten, 327, 821, doi: [10.1002/asna.200610655](https://doi.org/10.1002/asna.200610655)
- VanderPlas, J., Connolly, A. J., Ivezic, Ž., & Gray, A. 2012, in Proceedings of Conference on Intelligent Data Understanding (CIDU), pp. 47–54, 2012., 47–54, doi: [10.1109/CIDU.2012.6382200](https://doi.org/10.1109/CIDU.2012.6382200)
- York, D. G., Adelman, J., Anderson, John E., J., et al. 2000, AJ, 120, 1579, doi: [10.1086/301513](https://doi.org/10.1086/301513)